

## Towards standardisation of the out-of-plane permeability measurement for reinforcement textiles

Yong, A. X.H.; Endruweit, A.; George, A.; May, D.; Aksoy, Y. A.; Caglar, B.; Dransfeld, C.; Masania, K.; Yuksel, O.; More Authors

### DOI

[10.1016/j.compositesa.2024.108630](https://doi.org/10.1016/j.compositesa.2024.108630)

### Publication date

2025

### Document Version

Final published version

### Published in

Composites Part A: Applied Science and Manufacturing

### Citation (APA)

Yong, A. X. H., Endruweit, A., George, A., May, D., Aksoy, Y. A., Caglar, B., Dransfeld, C., Masania, K., Yuksel, O., & More Authors (2025). Towards standardisation of the out-of-plane permeability measurement for reinforcement textiles. *Composites Part A: Applied Science and Manufacturing*, 190, Article 108630. <https://doi.org/10.1016/j.compositesa.2024.108630>

### Important note

To cite this publication, please use the final published version (if applicable).  
Please check the document version above.

### Copyright

Other than for strictly personal use, it is not permitted to download, forward or distribute the text or part of it, without the consent of the author(s) and/or copyright holder(s), unless the work is under an open content license such as Creative Commons.

### Takedown policy

Please contact us and provide details if you believe this document breaches copyrights.  
We will remove access to the work immediately and investigate your claim.

***Green Open Access added to TU Delft Institutional Repository***

***'You share, we take care!' - Taverne project***

**<https://www.openaccess.nl/en/you-share-we-take-care>**

Otherwise as indicated in the copyright section: the publisher is the copyright holder of this work and the author uses the Dutch legislation to make this work public.



## Towards standardisation of the out-of-plane permeability measurement for reinforcement textiles

A.X.H. Yong<sup>a,\*</sup>, A. Endruweit<sup>b</sup>, A. George<sup>c</sup>, D. May<sup>d</sup>, Y.A. Aksoy<sup>e</sup>, M.A. Ali<sup>f</sup>, T. Allen<sup>g</sup>, P. Baral<sup>h</sup>, C. Betteridge<sup>c</sup>, C. Brauner<sup>i</sup>, B. Caglar<sup>e</sup>, A. Chiminelli<sup>j</sup>, D. Cracknell<sup>g</sup>, L. Dame<sup>c</sup>, J. Dittmann<sup>k</sup>, C. Dransfeld<sup>e</sup>, S. Drapier<sup>h</sup>, J.A. García Manrique<sup>l</sup>, E. Garrigou<sup>h</sup>, A. Guilloux<sup>m</sup>, P. Hubert<sup>n</sup>, J. Ivens<sup>o</sup>, J. Janzen<sup>d</sup>, T. Khan<sup>f</sup>, H. Kikuta<sup>p</sup>, K. Kind<sup>q</sup>, M. Laspalas<sup>j</sup>, J. Lee<sup>g</sup>, X. Liu<sup>q</sup>, M. Lizaranzu<sup>j</sup>, S.V. Lomov<sup>q</sup>, K. Masania<sup>e</sup>, V. Michaud<sup>s</sup>, P. Middendorf<sup>k</sup>, S. Miguel<sup>j</sup>, J. Muñoz<sup>l</sup>, S.S. Narayana<sup>n</sup>, C.H. Park<sup>p</sup>, G. Pedoto<sup>h</sup>, A. Pisupati<sup>p</sup>, D. Sayinbas<sup>r</sup>, P. Sousa<sup>o</sup>, M. Sozer<sup>r</sup>, J. Staal<sup>s</sup>, M. Steinhardt<sup>q</sup>, H. Teixido<sup>s</sup>, R. Umer<sup>f</sup>, J.D. Vincent<sup>a</sup>, V. Werlen<sup>i</sup>, O. Yuksel<sup>e</sup>

<sup>a</sup> National Physical Laboratory, UK

<sup>b</sup> University of Nottingham, UK

<sup>c</sup> Brigham Young University, USA

<sup>d</sup> Leibniz-Institut für Verbundwerkstoffe GmbH, Germany

<sup>e</sup> TU Delft, Netherlands

<sup>f</sup> Khalifa University of Science and Technology, United Arab Emirates

<sup>g</sup> University of Auckland, New Zealand

<sup>h</sup> Ecole des Mines St-Etienne, France

<sup>i</sup> FHNW University of Applied Sciences and Arts Northwestern Switzerland, Switzerland

<sup>j</sup> Aragon Institute of Technology (ITA), Spain

<sup>k</sup> University of Stuttgart, Germany

<sup>l</sup> Universitat Politècnica de Valencia, Spain

<sup>m</sup> TENSYS, France

<sup>n</sup> McGill University, Canada

<sup>o</sup> KU Leuven, Belgium

<sup>p</sup> IMT Nord Europe, France

<sup>q</sup> TU Munich, Germany

<sup>r</sup> Koc University, Turkey

<sup>s</sup> LPAC, Ecole Polytechnique Fédérale de Lausanne (EPFL), Switzerland

### ARTICLE INFO

#### Keywords:

Fabrics/textiles  
Permeability  
Process monitoring  
Liquid composite moulding  
Resin flow

### ABSTRACT

In the collaborative effort towards standardisation of out-of-plane permeability measurement, an international benchmarking exercise was carried out whereby 19 participants worldwide were instructed to measure the out-of-plane permeability following a number of strict guidelines, informed by the outcomes of the first international benchmarking exercise completed in 2021. This paper presents the results of the exercise and an assessment of the reproducibility of the data and the suitability of the proposed test method. The data returned were subjected to a number of statistical analysis methods, which showed that adherence to the test guidelines resulted in a high likelihood of a participant not being an outlier and therefore providing evidence that the test method proposed in this paper is a suitable way forward for a standardised test method.

\* Corresponding author.

E-mail address: [ana.yong@npl.co.uk](mailto:ana.yong@npl.co.uk) (A.X.H. Yong).

<https://doi.org/10.1016/j.compositesa.2024.108630>

Received 30 August 2024; Received in revised form 1 November 2024; Accepted 28 November 2024

Available online 30 November 2024

1359-835X/© 2024 Elsevier Ltd. All rights are reserved, including those for text and data mining, AI training, and similar technologies.

## 1. Introduction

Liquid Composite Moulding (LCM) processes are closed-mould, out-of-autoclave processes for the manufacture of composite components. They are based on the principle of injecting or infusing liquid resin into a dry fibrous reinforcement which has been preformed and positioned in a mould to achieve the desired shape. Relatively high fibre volume fractions and low void content, comparable to that obtained in autoclave processes using prepreg, can be obtained at relatively short cycle times if LCM processes are implemented appropriately. Hence, LCM processes have been adopted for industrial production of composite components, and a significant body of work on different aspects of the processes has been published [1–3].

The quality of components produced using LCM (in terms of complete reinforcement impregnation) and the process cycle time depend strongly on the flow of the liquid resin. At the component-scale, this is typically described by Darcy's Law [4], which although originally applied towards one-dimensional flow saturated with water, has since been generalized for a variety of porous media flow scenarios. A three-dimensional form of Darcy's Law can be expressed as

$$\mathbf{v} = -\frac{\mathbf{K}}{\mu} \nabla p \quad (1)$$

Here,  $\mathbf{v}$  is the phase-averaged flow velocity (of resin and fibres),  $\mu$  is the dynamic viscosity of the resin and  $\nabla p$  is the flow-driving pressure gradient. The permeability of the reinforcement,  $\mathbf{K}$ , indicates how easily the resin will flow through the reinforcement. It is a homogenised expression of the properties of the fibrous reinforcement, specifically the fibre volume fraction,  $V_f$ , and the geometry of pores between the individual fibres. Values of the permeability can be different in different material directions due to the anisotropy of the material. Therefore,  $\mathbf{K}$  is considered as a symmetrical second order tensor, which is fully characterised by three principal values (corresponding to three orthogonal directions). For thin fabric layers (where the continuous fibres are orientated mainly in-plane), the fibres and pores between them are aligned in one or more in-plane directions. The principal permeability directions coincide with the in-plane directions of the highest and the lowest flow velocity, and the out-of-plane (or through-thickness) direction of the fabric. For thick stacks from multiple fabric layers, regular offsets between the layers may result in a skewed permeability tensor, where the principal directions do not necessarily coincide with the fabric directions [5]. However, for stacks with purely stochastic layer offsets, the out-of-plane direction will coincide with a principal permeability direction. Typically, in-plane permeabilities are in the order of  $10^{-12} \text{ m}^2$  to  $10^{-9} \text{ m}^2$  [6–8] and out-of-plane (or through-thickness) permeabilities in the order of  $10^{-14} \text{ m}^2$  to  $10^{-12} \text{ m}^2$  [9].

As characterisation of the reinforcement permeability is important in the development of a process design which ensures the complete saturation of the dry reinforcement by the injected/infused resin and which minimises process cycle times, a wide variety of methods for permeability measurement has been implemented over time. Typically, these methods are based on solving Eq. (1) for the permeability and measuring the flow velocity, pressure gradient and resin viscosity. At present, most test methods used to measure the permeability, based on Darcy's Law, involve separate measurement of the in-plane and out-of-plane permeability. More rarely, the permeability is measured in three dimensions simultaneously (which requires a more complex data reduction scheme). Comprehensive overviews (and discussions) of test methods and data reduction schemes can be found in the literature [11,12]. As it had been observed in direct comparison that different test methods can result in different values for the obtained permeability of a given reinforcement at a given fibre volume fraction [13], a series of worldwide and regional benchmarking exercises have been conducted to establish the best-practice methods [6–10,14–17]. Eventually, a standard for measurement of the in-plane permeability was published in 2023 [18].

The work presented here was organised by the National Physical Laboratory in the UK (NPL) and reports on the efforts to understand the best-practice in measurement of the out-of-plane permeability and follows on from the first international benchmarking exercise completed in 2021 [9]. In the first exercise, participants were asked to measure the permeability of the same fabric at three prescribed (target) fibre volume fractions with no limitations on the procedure used. A large scatter (two orders of magnitude) was observed between data obtained by different participants. However, most results (65 out of 85 data points in total for a non-crimp fabric) lay in a much narrower band where the factor between minimum and maximum permeability values at any fibre volume fraction was approximately four. As 20 of the 26 participants had opted for a 1D saturated test method, this was recommended as the method to be used in this follow-up exercise. This method can be used to characterise the (out-of-plane) permeability normal to the specimen surface. This will typically coincide with a principal permeability direction, although this is not necessarily the case (for specimens with skewed permeability tensor [5]). To minimise the variability in permeability data, detailed guidelines for the experiments were provided to the 19 participants (Table 1) in this exercise. Data obtained using methods not compliant with these guidelines were accepted but deviations resulting from the noncompliance will be illustrated in this study.

Aiming to obtain consistent permeability data between laboratories, this new exercise was to establish a defined test procedure for the out-of-plane permeability and quantify the repeatability and reproducibility of results, which will then be turned into a test standard.

## 2. Materials

The textile reinforcement material used in this study was the Saertex X-E biaxial ( $\pm 45^\circ$ ) E-glass fibre non-crimp fabric (Fig. 1) with a nominal areal weight of  $444 \text{ g/m}^2$  ( $217 \text{ g/m}^2$  in  $+45^\circ$  and in  $-45^\circ$  direction and additionally  $1 \text{ g/m}^2$  and  $2 \text{ g/m}^2$  in  $0^\circ$  and  $90^\circ$ , respectively, for stabilization) as well as  $6 \text{ g/m}^2$  polyester stitching yarn (76 dtex) with a warp pattern at a stitch length of 2.6 mm and a gauge length of 5 mm. This material was nominally the same as that used in the previous benchmarking exercises for out-of-plane permeability measurement, in-plane permeability measurement and compressibility measurement. However, the material was from a different batch, which means that the properties were not necessarily the same as in the previous studies. The average bundle width, stitches spacing, and bundle gap for this batch were  $1.97 \text{ mm} \pm 0.20 \text{ mm}$ ,  $5.12 \text{ mm} \pm 0.18 \text{ mm}$ , and  $0.45 \text{ mm} \pm 0.09 \text{ mm}$ , respectively. The textile was prepared by the manufacturer and

**Table 1**  
List of participants.

Participant	Institution	Country
1	KU Leuven	Belgium
2	McGill University	Canada
3	Ecole des Mines St-Etienne	France
4	IMT Nord Europe	France
5	TENSYL	France
6	Leibniz-Institut für Verbundwerkstoffe	Germany
7	ITA Aragon Institute of Technology	Spain
8	TU Munich	Germany
9	University of Stuttgart	Germany
10	TU Delft	Netherlands
11	University of Auckland	New Zealand
12	Universitat Politècnica de Valencia	Spain
13	Ecole Polytechnique Fédérale de Lausanne	Switzerland
14	FHNW University of Applied Sciences and Arts Northwestern Switzerland	Switzerland
15	Koc University	Turkey
16	Khalifa University of Science and Technology	UAE
17	National Physical Laboratory	UK
18	University of Nottingham	UK
19	Brigham Young University	USA

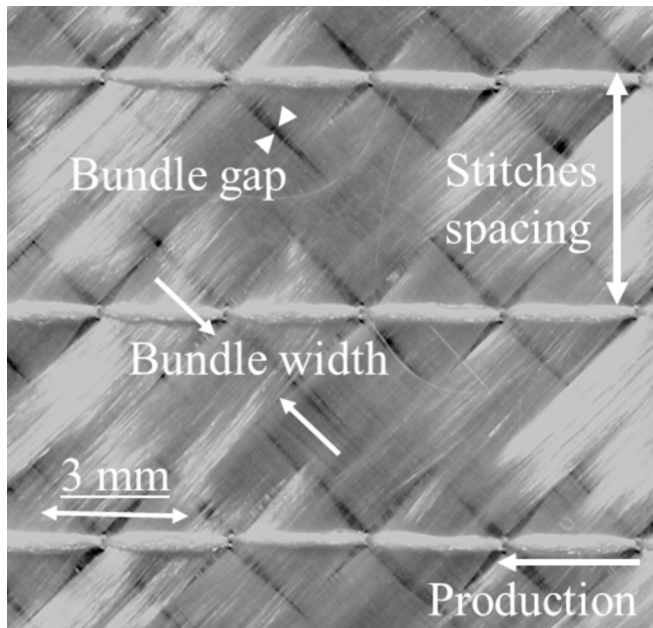


Fig. 1. Image of the textile characterized in this benchmark study (reprinted from [8]).

distributed by NPL to all participants on rolls. Cutting and stacking was done by the participants.

The test fluid used in this exercise was the Dow Corning Xiameter PMX-200 100 cs silicone oil, which again was the same as the fluid specified for the previous benchmarking exercises. Participants were asked to measure the viscosity of the batch of test fluid used at their site or use reference data for the viscosity as a function of the temperature previously acquired by TU Munich [8]. Viscosity measurements will be detailed later in this paper, in Section 5.2.

### 3. Methods

The procedure used in this study was designed following the outcomes of the first international benchmarking exercise and also taking into account the lessons learned from the in-plane permeability and compressibility benchmarking exercises. In this second exercise, the following test parameters were mandatory:

- Tests could be saturated or unsaturated, provided the 1D test method was used (as illustrated in Fig. 2a and b). Although it is well known that the mechanisms of flow differ between both test methods [19,20], both were accepted as there is no clear indication if permeability values obtained using saturated methods are greater, smaller, or the same as those from unsaturated methods [21]. The purpose of the previous and current benchmarking exercises was to establish a recommended test method for standardisation. The first benchmarking exercise showed that the 1D test method was by far the most popular and consistent in concept, where only a small number of organisations measure the out-of-plane permeability using the 3D test method and there was no consistency in the equipment design or equations used. Tests were conducted at three defined fibre volume fractions, VF, with target values: 46 %, 50 % and 54 %. Permeability has been shown to be highly sensitive to fibre content [6–8]. These volume fractions are representative of the range typically used in manufacturing of real composite products. Targeting three values allows better inter-participant comparison of permeability values. The actual values for each test were determined by the participants by weight of each specimen. Five tests were conducted at each target fibre content value.
- Specimens were to consist of a fabric stack of no less than 10 and no more than 20 individual layers, all stacked with equal orientation. Participants were provided with a range to ensure that the mandatory volume fractions were achievable within any limitations caused by the individual test setup. Setting the sample thickness is often only possible in discrete steps (specifically, if spacers are used). A minimum of 10 layers was set in order to minimise the impact of local volume fraction changes caused by the presence of the perforations in the parts of the tool in contact with the specimen. Prescribing a minimum number of layers for the tests generally also helps to reduce variability in the measured permeabilities resulting from random nesting (or layer shifts in the absence of nesting) between individual fabric layers, which has been shown in previous studies to decrease significantly with increasing number of layers [22,23]. The maximum of 20 was set in order to minimise potential sample preparation errors such as edge sealing inconsistencies, layer count and stacking variability.
- Specimens were to have an edge length (if square) or diameter (if round) in the order of 100 mm. Dimensions of this order ensure that the area of the specimens covers several complete fabric unit cells, even for fabrics with complex architecture and large unit cells. A minimum size is recommended, as the ratio of edge length to specimen area decreases with increasing dimensions, which reduces the risk of potential edge effects having a large influence on the results. The recommended edge length also accounts for the practical limitations to using larger specimens (as specimens with dimensions in the order of 1 m would be difficult to handle, and suitable test set-ups would be difficult to operate).
- Specimens were to be cut with a precise method such as a CNC cutter or die cutter. Precision cutting of the specimen edges was required to ensure minimal fraying and shear. Fraying or shear of the specimen could cause a change in the porosity and therefore permeability of the specimen. It also hampers the contact between the specimen and

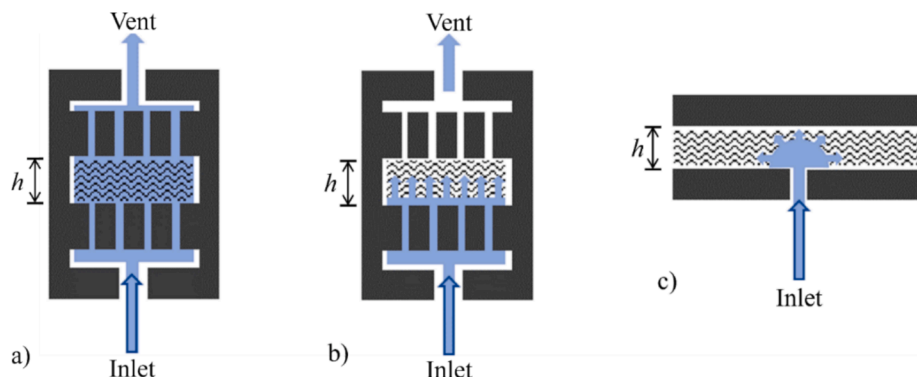


Fig. 2. Schematic diagrams of the principles of measurement in a) 1D saturated flow, b) 1D unsaturated flow, and c) 3D unsaturated flow [9].



the tool used for the flow experiments, as a non-uniform edge is more difficult to seal.

- Pressure and flow rate were to be measured independently of set (target) values to ensure an accurate input into the calculation of the permeability using a form of Eq. (1). This is essential, as true values may deviate from set values. Differences in pressure can be caused by losses in the pipes between pressure pot or pump and tool inlet. If a flow rate is set, this may be affected by a pressure build-up on the upstream side of the tested specimen. Depending on the tool design, there may be a pressure build-up in the tool downstream of the specimen, meaning that the pressure in a vented tool may not necessarily be atmospheric.
- Participants were to employ an edge-sealing procedure, such as the use of a sealant paste or O-ring, to prevent gaps from forming between specimen and tool. This aims to minimise the risk of race-tracking of the fluid around the edge of the specimen [24], i.e. faster flow through gaps than through the specimen, which would result in an overestimation of the specimen permeability. If the application of sealant reduces the effective flow channel cross-section in 1D experiments, this needs to be considered in permeability calculation (according to Eq. (2) below).
- The (negative) pressure difference,  $\Delta p$ , between the fluid inlet (typically at the bottom surface of the specimen) and the fluid outlet (typically at the top surface) was to be between  $-100$  kPa and  $-200$  kPa during testing. These limits were chosen as lower absolute values of  $\Delta p$  may lead to higher relative uncertainty in measured values (at given accuracy of the measurement method). In addition, any unsaturated test would be affected to a greater extent by wetting effects at lower absolute pressure differences [25,26]. On the other hand, higher absolute pressure differences may lead to hydrodynamic compaction of the reinforcement [27–29], causing significant changes in the reinforcement microstructure. This would affect both the true fibre volume fraction and the permeability, resulting in a misrepresentation of the dependence of  $K_z$  on  $V_f$ . Observations from saturated 1D flow experiments at an absolute pressure difference  $\Delta p = 100$  kPa indicate that, for the same NCF characterised here, the specimen thickness was reduced by approximately 1.1 %, 0.3 % and 0.3 % at target fibre volume fractions of 46 %, 50 % and 54 %, respectively [9]. Hence, the effect of hydrodynamic compaction on fibre volume fraction and permeability can be expected to be small in the range of pressure values prescribed here.

Of the 19 participants in this study, 2 used the 3D test method and 17 used the 1D test method. Additional details for the 3D test methods have been provided in the [supplementary documents](#). Schematic diagrams of the different types of test configuration are given in [Fig. 2](#). The 1D test setup consists of a stiff flow channel within which the specimens are held between two perforated platens at a known thickness that correlates with the chosen  $V_f$ . These platens are perforated to allow fluid to flow through the specimen between the inlet and outlet. For the purposes of this work, no specifications were given for the size and number of perforations. In saturated flow experiments, the constant pressure drop and constant flow rate are measured once steady-state flow has developed. Using the saturated 1D test method, the out-of-plane permeability,  $K_z$ , can be calculated using Darcy's Law in the following arrangement:

$$K_z = -\frac{Q\mu t}{A\Delta p} \quad (2)$$

Here,  $Q$  is the volumetric flow rate,  $A$  is the cross-sectional area of the flow channel,  $\mu$  is the fluid viscosity,  $\Delta p$  is the difference between fluid pressures measured at or close to the inlet and outlet, and  $t$  is the thickness of the specimen. The thickness of the specimen is taken as the distance between the platens which hold the fabric stack in position under compression. All 17 participants using a 1D test setup used the saturated test method and 2 of these participants submitted additional

data collected using the unsaturated test method. Measurements carried out using the 3D test method use separate equations for calculation of the permeability [30].

The fibre volume fraction corresponding to a measured permeability value was determined according to

$$V_f = \frac{m}{\rho t A} \quad (3)$$

Here, the mass,  $m$ , was obtained by weighing each specimen. For the density of the glass fibres,  $\rho$ , a value of  $2550 \text{ kg/m}^3$  was given.

[Table 2](#) shows a breakdown of the test setup for each individual participant. [Table 3](#) shows the details of the measurements taken for permeability calculation. [Table 4](#) shows the details of the specimen preparation for each participant.

[Table 5](#) summarises the compliance of the different test series with the guidelines. Out of all 21 submitted test series, 11 series comply with all guidelines.

## 4. Results

### 4.1. Introduction to analysis

This section provides a presentation of the results returned by the participants, followed by analysis using a number of statistical methods. The initial data presented are the  $K_z$  values alongside the corresponding  $V_f$  values at which they were measured for all data returned ([Section 4.2](#)). Subsequently, two methods of statistical analysis were carried out to identify outliers in the data. These were (1) the method outlined in ASTM E691, which was created for the specific purpose of calculating the precision of data in interlaboratory trials and (2) Thomson-Tau analysis, as used in the previous benchmark study [9].

As is shown in the next section, the data returned by participants deviated from the three  $V_f$  target values prescribed in the guidelines for this study, therefore it was necessary to reduce the number of variables from two ( $K_z$  and  $V_f$ ) to one, prior to carrying out any statistical analysis. Here, three different methods were applied:

- Adjustment of the  $K_z$  to a common  $V_f$  using the Kozeny-Carman (KC) fit model [31] which expresses the following relationship between  $V_f$  and  $K_z$ :

**Table 2**  
Details of the test setup for each participant.

Participant ID	Flow	Test geometry	Flow controlled or pressure controlled	Edge sealing method
1	Unsaturated	3D	Set pressure	None
2	Saturated	1D	Set pressure	O-ring
3a	Saturated	1D	Set flow	Clamping
3b	Unsaturated	1D	Set flow	Clamping
4	Saturated	1D	Set pressure	Sealant
5	Saturated	1D	Set pressure	Clamping
6	Saturated	1D	Set pressure	Clamping and sealant
7	Saturated	1D	Set pressure	O-ring
8	Saturated	1D	Set pressure	O-ring
9a	Saturated	1D	Set pressure	O-ring
9b	Unsaturated	1D	Set pressure	O-ring
10	Saturated	1D	Set pressure	O-ring
11	Saturated	1D	Set pressure	Sealant
12	Saturated	1D	Set pressure	Sealant
13	Saturated	1D	Set pressure	Sealant
14	Saturated	1D	Set pressure	Sealant
15	Saturated	1D	Set pressure	Clamping
16	Saturated	1D	Set flow	Sealant
17	Saturated	1D	Set pressure	Sealant
18	Saturated	1D	Set flow rate	Sealant
19	Unsaturated	3D	Set flow	None

**Table 3**  
Details of the measurement and sensing methods for each participant.

Participant ID	Thickness measurement	Pressure sensor location		Flow measurement method
		Inlet	Outlet	
1	Laser sensors	At pot	None	Etched fibre sensors
2	Stepper motor movement	At tool	None	Mass loss from pot
3a	Spacer thickness	At tool	None	Video of flow front
3b	Spacer thickness	At tool	None	Thermocouples in specimen
4	Spacer thickness	At tool	At tool	Flow meter
5	Spacer thickness	At tool	At tool	Not known
6	Spacer thickness	At tool	At tool	Flow meter
7	Ruler/Caliper	At tool	At tool	Mass loss from pot
8	Video extensometer	At tool	At tool	Mass loss from pot
9a	Video extensometer	At pot	At tool	Flow meter
9b	Video extensometer	At pot	At tool	Flow meter
10	Machine displacement*	At tool	At tool	Mass gain at outlet
11	Machine displacement*	At tool	At tool	Mass loss from pot
12	Not known	At tool	None	Not known
13	Spacer thickness	In-line	In-line	Mass loss from pot
14	Spacer thickness	At tool	At tool	Mass loss from pot
15	Ruler/Caliper	In-line	In-line	Mass loss from pot
16	Spacer thickness	At tool	At tool	Flow meter and mass loss
17	Machine displacement*	At tool	At tool	Mass loss from pot
18	Spacer thickness	At tool	At tool	Flow meter
19	Spacer thickness	At pot	None	Visual inspection

\* Test rig mounted in universal testing machine.

$$K_z = k_0 \frac{(1 - V_f)^3}{V_f^2} \quad (4)$$

- $K_z$  within a  $V_f$  interval range (bin).
- Comparison of one single descriptor for each data set, the constant  $k_0$  from the KC fit curve.

Using these methods, statistical analysis was applied initially to all datasets (1D saturated, 1D unsaturated, and 3D unsaturated), and subsequently a reduced number of datasets which excluded all test methods except 1D saturated, and data which did not meet the standard for the known relationship of increasing  $K_z$  with decreasing  $V_f$ . It is to be noted that Eq. (4) is a phenomenological model which is often used successfully but may not always fit experimental data with high accuracy. More physics-based models exist only for aligned fibres arranged in regular patterns [32,33], which means they are not applicable here where the entire textile reinforcement is studied.

#### 4.2. Summary of results

Including submissions from participants 3 and 9 for both saturated and unsaturated 1D tests and from participants 1 and 19 for tests carried

out using a 3D test setup, 21 data sets were submitted in total (Fig. 3). Here, each data point represents the average of the 5 test repeats carried out by each participant (with the exception of participant 1, who conducted three repeat tests). The laboratories that complied with the guidelines are delineated from the ones who did not comply by using solid and hollow markers, respectively. It seems that the non-compliant data points are on the periphery of all data points, i.e. several high permeability and high fibre content points which appear as possible outliers are also non-compliant points.

A difficulty in carrying out a thorough statistical analysis of the data is the dependence of the permeability on the fibre volume fraction, which means that permeability values obtained at different fibre volume fractions are not directly comparable. A KC fit curve according to Eq. (4) can be created for all data points in Fig. 3, where  $k_0 = 3.13 \times 10^{-12} \text{ m}^2$ . As the scatter in the data is high, the coefficient of correlation is low at the value of  $R^2 = 0.255$ .

Fig. 3 clearly shows that the scatter of the fibre volume fraction, which results from different numbers of layers (i.e. specimen mass) and different specimen thicknesses being used, extends beyond the target values of 46 %, 50 % and 54 % requested in the guidelines. The lowest  $V_f$  (target value of 46 %) varied between 40 % and 52 %, the intermediate  $V_f$  (target value of 50 %) between 48 % and 57 %, and the highest  $V_f$  (target value of 54 %) between 53 % and 61 %. Without taking this variation in fibre volume fraction into account, the coefficient of variation (c.v.) of the average permeability values at each target  $V_f$  of 46 %, 50 % and 54 % is 182 %, 174 % and 168 %, respectively. The range in average permeability values for each fibre volume fraction was similar to that of the first benchmark study [9].

Within the data for each individual participant, the c.v. of  $K_z$  varied between 2 % and 96 % at a target  $V_f$  of 46 %, between 4 % and 60 % at a target  $V_f$  of 50 %, and between 4 % and 63 % at a target  $V_f$  of 54 %. The average c.v. within each data set at each target  $V_f$  is 16 %, 16 % and 15 %, respectively.

#### 4.3. Comparison at equal fibre volume content

To enable the comparison of the permeability values despite the variation in fibre volume fraction, each measured permeability value  $K_z$  was adjusted to the equivalent permeability  $K_{z,e}$  at the target fibre volume fraction,  $V_{f,e}$  (46 %, 50 %, and 54 %), by the following equation:

$$K_{z,e} = K_z \left( \frac{1 - V_{f,e}}{1 - V_f} \right)^3 \left( \frac{V_f}{V_{f,e}} \right)^2 \quad (5)$$

This equation results from solving Eq. (4) for the KC constant using given values of  $K_z$  and  $V_f$ , then substituting the derived expression for  $k_0$  in Eq. (4) for  $K_{z,e}$  and  $V_{f,e}$ . The validity of this method depends upon the fit quality of the KC model to each participant's data set, which varied between participants. Application of Eq. (5) allowed conversion of all the permeability data to each of the three target fibre volume fractions (Fig. 4). A KC model was fit to all of the fitted data, as was done for Fig. 3, and results in the same value  $k_0 = 3.13 \times 10^{-12} \text{ m}^2$ , with  $R^2 = 0.276$ . The high permeability non-compliant outliers are again seen as in Fig. 3.

#### 4.4. ASTM analysis of outliers

Based on all submitted data (Fig. 3), ASTM standard E691 [34] was used to evaluate the consistency of the adjusted permeability measurements and to look for statistical outliers. Both between-laboratory consistency,  $h$ , and within-laboratory consistency,  $k$ , were calculated, where  $h$  is the deviation of the lab average from the average of all lab averages divided by the standard deviation of those averages, and  $k$  is the standard deviation for one laboratory's data divided by the standard deviation of all labs' standard deviations. The consistency values are plotted for each target fibre volume fraction and participant in Fig. 5. With 21

**Table 4**

Details of the specimen preparation and geometry for each participant;  $l$  and  $w$  indicate the length and width of rectangular specimens;  $d$  indicates the diameter of round specimens.

Participant ID	Fabric cutting method	Specimen geometry	Specimen dimensions / mm			Number of layers in stack		
			$l$	$w$	$d$	$V_{f1}$	$V_{f2}$	$V_{f3}$
1	Scissors	Square	250	250	–	25	25	25
2	Die cutter	Circle	–	–	76.2	10	10	10
3a	Die cutter	Circle	–	–	98	13	11	10
3b	Die cutter	Circle	–	–	98	13	11	10
4	Scissors	Square	169	169	–	6	6	6
5	Die cutter	Circle	–	–	100	14	13	12
6	CNC Cutter	Ellipse	155	192	–	13	12	11
7	Die cutter	Circle	–	–	60	15	14	12
8	Die cutter	Circle	–	–	124	10	10	10
9a	CNC Cutter	Square	79	79	–	20	20	20
9b	CNC Cutter	Square	79	79	–	20	20	20
10	CNC Cutter	Circle	–	–	100	20	20	20
11	Die cutter	Circle	–	–	130	15	15	15
12	Laser	Circle	–	–	140	10	10	10
13	Scissors	Circle	–	–	120	14	13	12
14	Die cutter	Circle	–	–	80	14	13	12
15	CNC Cutter	Circle	–	–	90	12	12	12
16	Die cutter	Circle	–	–	150	13	11	10
17	Die cutter	Circle	–	–	132	10	11	12
18	Die cutter	Circle	–	–	80	12	11	10
19	Knife	Square	150	150	–	40	37	24

**Table 5**

Details of whether or not participants complied with the test procedure as outlined in Section 3.

Participant ID	1D Test geometry	10–20 layers	Area in 100 mm scale	Fabric cutting	Stand alone sensors	Pressure differential	Edge sealing	Target $V_f$ used	Overall score
1	No	No	Yes	No	No	No	No	Yes	No
2	Yes	Yes	Yes	Yes	Yes	Yes	Yes	Yes	Yes
3a	Yes	Yes	Yes	Yes	Yes	Yes	No	Yes	No
3b	Yes	Yes	Yes	Yes	Yes	Yes	No	Yes	No
4	Yes	No	Yes	No	Yes	No	Yes	Yes	No
5	Yes	Yes	Yes	Yes	Yes	Yes	Yes	No	No
6	Yes	Yes	Yes	Yes	Yes	Yes	Yes	Yes	Yes
7	Yes	Yes	Yes	Yes	Yes	Yes	Yes	Yes	Yes
8	Yes	Yes	Yes	Yes	Yes	Yes	Yes	Yes	Yes
9a	Yes	Yes	Yes	Yes	Yes	No	Yes	Yes	No
9b	Yes	Yes	Yes	Yes	Yes	Yes	Yes	Yes	Yes
10	Yes	Yes	Yes	Yes	Yes	Yes	Yes	Yes	Yes
11	Yes	Yes	Yes	Yes	Yes	Yes	Yes	Yes	Yes
12	Yes	Yes	Yes	No	Yes	No	Yes	Yes	No
13	Yes	Yes	Yes	No	Yes	Yes	Yes	No	No
14	Yes	Yes	Yes	Yes	Yes	Yes	Yes	Yes	Yes
15	Yes	Yes	Yes	No	Yes	No	Yes	No	No
16	Yes	Yes	Yes	Yes	Yes	Yes	Yes	Yes	Yes
17	Yes	Yes	Yes	Yes	Yes	Yes	Yes	Yes	Yes
18	Yes	Yes	Yes	Yes	Yes	Yes	Yes	Yes	Yes
19	No	No	Yes	No	No	Yes	No	Yes	No

total complete sets of data, and 5 repeats for each fibre volume fraction, the outlier threshold values for  $h$  and  $k$  are  $\pm 2.57$  and  $1.88$ , respectively, at a significance level of  $0.5\%$  [34]. As seen in Fig. 5, values at all three fibre volume fractions for participant 12 exceed the positive  $h$  outlier threshold. As the source of this inconsistency could not be identified based on the information provided by the participant, and repeating the tests was not possible in this study, the identified outlier was excluded from the remaining analysis.

The  $h$  and  $k$  values were then re-calculated based on the remaining 20 data sets. It is to be noted that the outlier thresholds also need to be updated if the number of data sets changes [34]. With removal of the skewed data from participant 12, the consistency values of the remaining participants increase. Values at all three  $V_f$  for participant 9a, and the value at  $V_f = 46\%$  for participant 19 then exceeded the positive  $h$  outlier threshold, suggesting their exclusion. The next iteration of calculations suggested exclusion of 9b by surpassing the  $k$  outlier

threshold for the value at  $V_f = 46\%$ , suggesting overly high inconsistency within that participant's data. The subsequent iteration did the same but for participant 1, suggesting its exclusion. This finally led to 16 remaining participant data sets lying within the outlier thresholds (Fig. 6).

For comparison, the ASTM outlier analysis was performed on the submitted data again, but now focussing only on the 1D saturated test results (i.e. ignoring results from 1D unsaturated or 3D methods) and excluding data showing an implausible increase in permeability with increasing fibre volume fraction. Data obtained using the 1D and 3D unsaturated test methods was reported in the first round of analysis for comparison, however the mechanisms of flow through a dry textile differ from those of a saturated textile due to capillary effects and the effects of dual-scale flow through dry textiles [19–21]. Due to the low number of datasets and the fundamental differences between the test methods, all unsaturated test data are excluded from this point onwards.



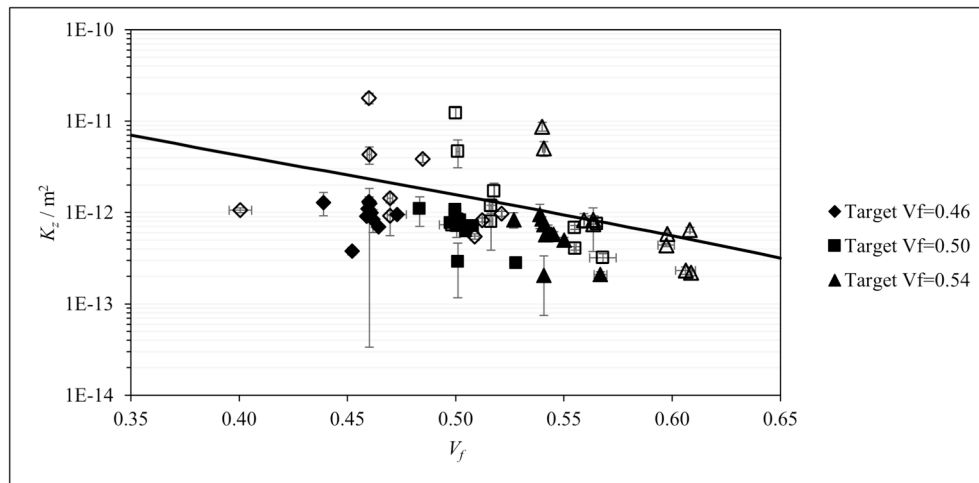


**Fig. 3.** All submitted permeability results (21 data sets with three data points each). Error bars indicate standard deviations. Solid and hollow markers respectively denote compliance and non-compliance with the guidelines. A KC fit curve is shown where  $k_0 = 3.13 \times 10^{-12} \text{ m}^2$  with  $R^2 = 0.255$ .

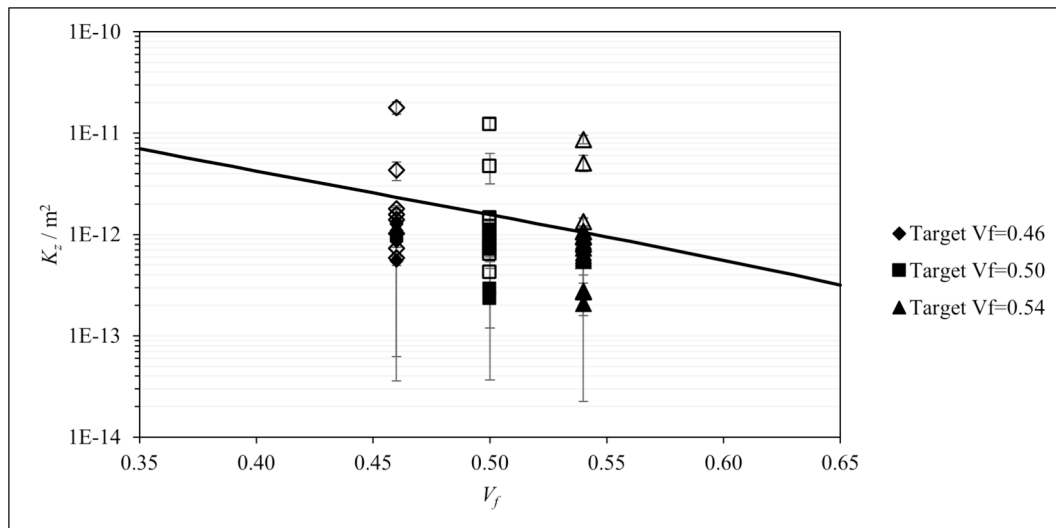


**Fig. 4.** Average permeability after adjustment of each experimental value to equivalent permeability at each target fibre volume fraction using Eq. (5). Solid and hollow markers respectively denote compliance and non-compliance with the guidelines. A KC fit curve is shown where  $k_0 = 3.13 \times 10^{-12} \text{ m}^2$  with  $R^2 = 0.276$ .

For the remaining 15 data sets, the outlier threshold values for  $h$  and  $k$  are  $\pm 2.47$  and  $1.86$ , respectively. Participant 12 is identified as an outlier as  $h$  values exceed the positive threshold at all three fibre volume fractions, i.e. the data set is inconsistent with the other participants' data. After that outlier is removed, all participants' data lies within the thresholds for both  $h$  and  $k$  (Fig. 7).

#### 4.5. Thomson Tau analysis of outliers

Adjusting measured permeability values to equivalent permeabilities at a target fibre volume fraction using the KC model (as described in Section 4.2) is generally regarded as a meaningful method of comparison, as was included in the ISO standard for in-plane permeability measurement [18]. Nevertheless, it can induce additional uncertainty, especially with the not yet standardised out-of-plane permeability tests, where the correlation between permeability and fibre volume fraction might be affected by systematic errors. Therefore, the Thompson-Tau test was applied to identify outliers as an alternative to the ASTM method, as it is easier to apply without using a fitting procedure. It was applied to data points, i.e. average permeability values at average fibre volume fractions based on five repeat tests, remaining after exclusion of

data from unsaturated 1D tests, 3D tests and those from data sets showing an increase in permeability with increasing fibre volume fraction. As permeability values were determined at different fibre volume fractions, the range of  $V_f$  between 0.40 and 0.64 was divided into bins (i.e. intervals of  $V_f$ ) with a width  $\Delta V_f = 0.04$ . For each bin, the change in  $K_z$  with  $V_f$  was assumed to be negligible. The Thompson-Tau test was applied iteratively to each bin, and outliers were excluded after each iteration. After 3 iterations, no more outliers were found (6 out of 45 data points were excluded). It is to be noted that the elimination depends strongly on the definition of the bins. Here, some bins contained only a small number of data points, and no data were eliminated (e.g. there were only two data points in the bin from 0.40 to 0.44) although some data points appear to be outliers (e.g. the data point at  $V_f = 0.40$ ). The remaining data points, which are plotted in Fig. 8, can be described by a KC fit with a coefficient  $k_0 = 1.51 \times 10^{-12} \text{ m}^2$ . Most non-compliant data points seem to be on the periphery.

Both the ASTM outlier analysis and the Thompson-Tau test using bins are based on individual data points rather than data series. As an alternative approach to identify and exclude outliers, a KC curve was fitted to each data set, and the Thompson-Tau test was applied to the coefficients,  $k_0$ , of all fit curves. This does not require adjusting  $K_z$  data

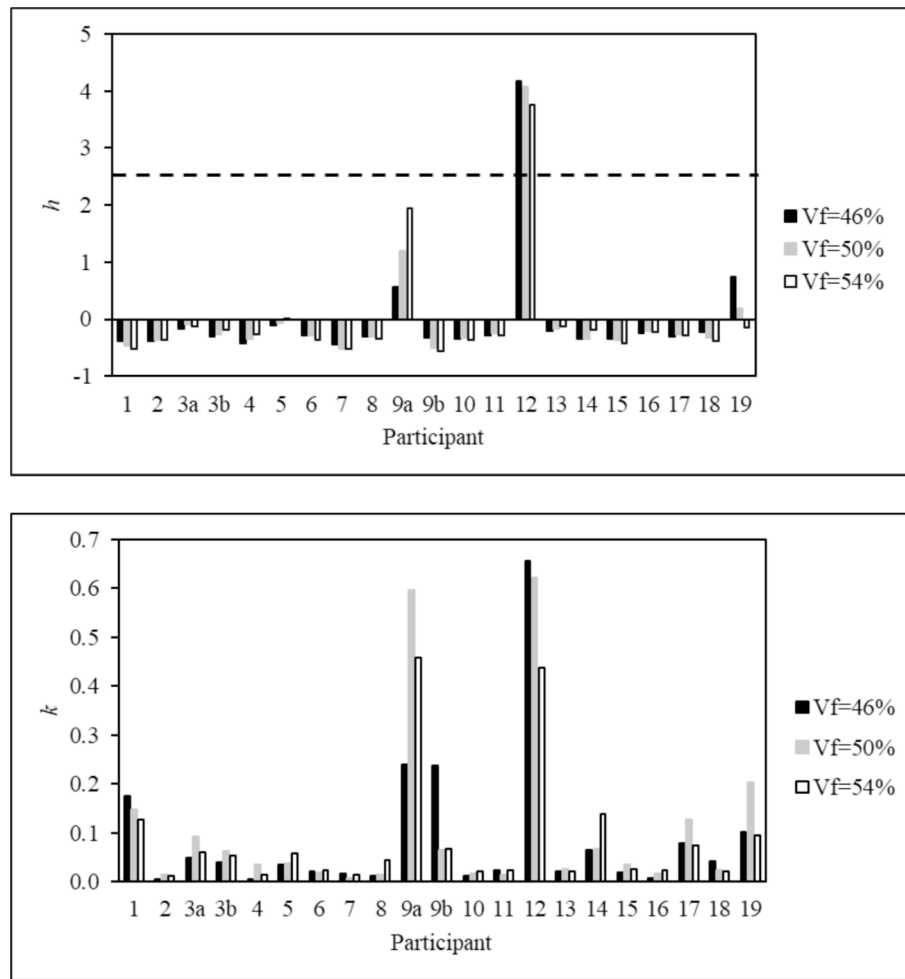


Fig. 5. Between-laboratory consistency,  $h$ , and within-laboratory consistency,  $k$ , for average adjusted permeability values at each target fibre volume fraction. Dashed line represents outlier threshold.

to target values of  $V_f$  or introducing bins for ranges of  $V_f$ , both of which may influence the results of the outlier analysis. After 3 iterations, no more outliers were found (4 out of 15 data sets, i.e. 12 out of 45 individual data points, were excluded). The data points corresponding to the remaining data series (Fig. 9) can be described by a KC fit with a coefficient  $k_0 = 1.44 \times 10^{-12} \text{ m}^2$ . Here, elimination depends on the assumption that each data set can be described with good accuracy by a KC fit. If the KC fit is not a very good approximation and the series is then represented by the individual data points, some of the data points may still appear to be outliers, although the corresponding  $k_0$  was not eliminated. Again, most non-compliant data points seem to be on the periphery.

## 5. Discussion

### 5.1. General observations

Table 6 relates the compliance with the guidelines for  $K_z$  testing to the results of the ASTM outlier analysis based on all data (ASTM 1), the results of the ASTM analysis focusing on data from 1D saturated tests and ignoring implausible results (ASTM 2), the results of the Thompson-Tau test based on  $V_f$  bins for individual data points (Ttau bins), and results of the Thompson-Tau test based on  $k_0$  for the data series (Ttau KC). The table shows the following:

- Both data sets from 3D test geometries are identified as outliers in the ASTM analysis on all 21 submitted data sets.

- One data set from 1D unsaturated test is identified as outlier in the ASTM analysis on all submitted data sets, while the other 1D unsaturated data set passes this outlier test. Interestingly, the data set identified as outlier is compliant with all guidelines, the data set that passes the test does not comply with all guidelines.
- Two data sets from 1D saturated tests are identified as outliers in the ASTM analysis on all submitted data sets. Both are not compliant with all guidelines. These two data sets can be visually identified as the two high outliers in Figs. 3 and 4.
- One data set showing an implausible increase in permeability with increasing fibre volume fraction is not identified as an outlier in the first ASTM analysis. This implies that considering individual data points at different (target) fibre volume fractions only and ignoring trends within the data sets is not sufficient for outlier identification.
- After the data sets from 3D tests, from 1D unsaturated tests and implausible data are excluded from the analysis, the second ASTM analysis returns the same outlier as the first ASTM analysis from the remaining 15 data sets.
- Both approaches using the Thompson-Tau test to identify outliers in the 15 remaining data sets give generally consistent results. The same 11 data sets pass the test using both approaches, and the same 3 data sets are identified as outliers. In one case, a data set is identified as outlier based on the  $k_0$  analysis, although it has passed the bin test.
- Comparing the second ASTM test to the Thompson-Tau tests, the same results are returned for 12 data sets. Three data sets failed at

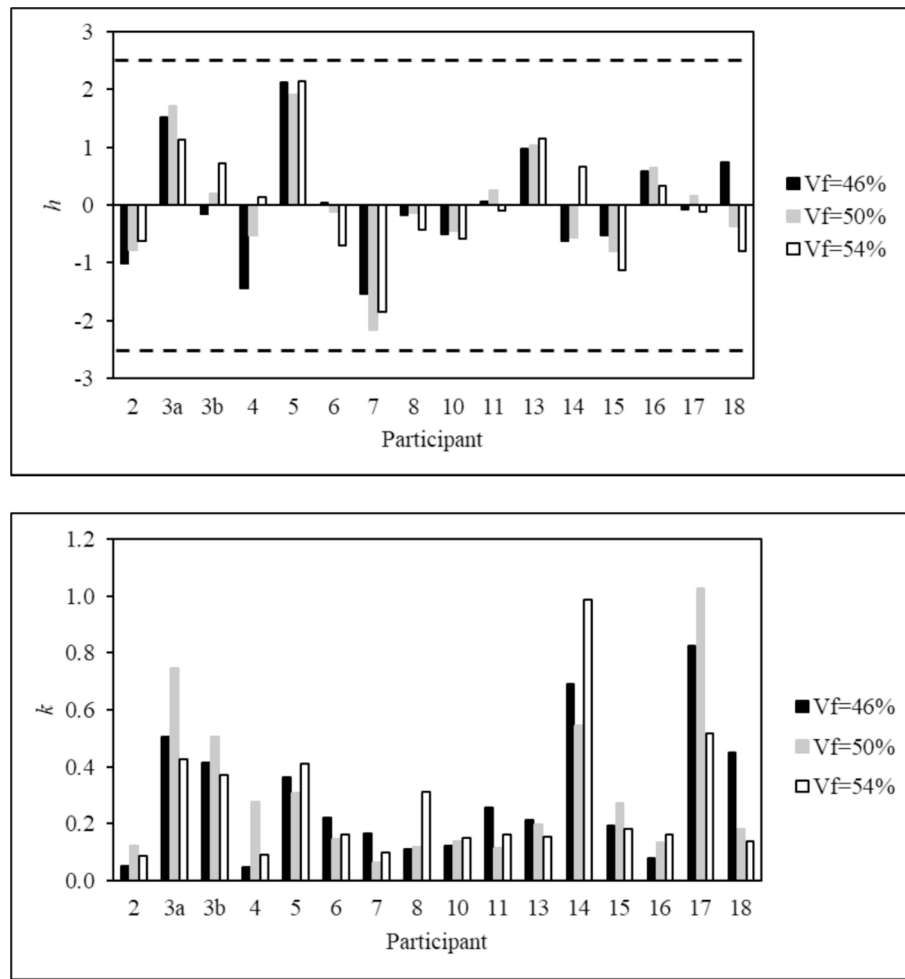


Fig. 6. Consistency measurements  $h$  and  $k$  after exclusion of outliers. Dashed lines represent outlier threshold.

least one of the Thompson-Tau tests, although they passed the ASTM test.

- Of the 15 data sets obtained in 1D saturated tests which do not show implausible behaviour,
  - o 8 are compliant with all guidelines and pass all tests,
  - o 3 are not compliant with all guidelines and fail at least one test,
  - o 3 are not compliant and pass all tests,
  - o 1 is compliant and fails at least one test.

The last observation in this list indicates that in 11 out of 15 data sets, non-compliance or compliance with the guidelines determines directly if a data set is identified as an outlier or not. For data sets not complying with all guidelines, it is still possible to pass all tests (3 out of 6 non-compliant data sets). For data sets complying with all guidelines, it is not likely to be identified as outlier (1 out of 9 compliant data sets). This means that the probability of being consistent with others is 50 % for non-compliant data sets, whilst it is 89 % for compliant data sets. Hence, it can be recommended to adhere to the proposed guidelines to minimise the risk of occurrence of outliers and maximise the chance of obtaining comparable data between laboratories. This also shows that the guidelines developed provide a suitable basis for standardisation.

## 5.2. Effect of viscosity measurement

For this study, the participants were asked to either measure the viscosity of the test fluid in a relevant temperature range themselves or use a reference curve provided by TU Munich. The reference curve was acquired on an Anton Paar MCR 302 rheometer with a cone and plate

geometry (25 mm diameter). At a rotational speed of 16.81/min (corresponding to a shear rate of 100/s), the temperature was ramped from 15 °C to 60 °C and back. The averaged data for the viscosity as a function of the temperature (Fig. 10) can be approximated with good accuracy (coefficient of correlation  $R^2 = 0.992$ ) by the curve

$$\mu = -45.83 \text{ mPa.s} \ln(T / ^\circ\text{C}) + 235.58 \text{ mPa.s} \quad (6)$$

Out of all participants in this study, fourteen participants carried out their own viscosity characterisation, while five participants used the provided reference curve. Test temperatures and fluid viscosities were reported together with the permeability data. Compared with the viscosities according to Eq. (6) at the reported test temperatures, the viscosity values reported by the participants were on average

- within  $\pm 10$  % for 13 participants,
- between 10 % and 20 % higher for three participants,
- between 20 % and 30 % higher for two participants,
- approximately 75 % higher for one participant.

This means that for approximately one third of the participants, the deviation in viscosity from the reference was greater than 10 %. As the permeability is derived from the recorded experimental data using Eq. (2), deviations in the measured viscosity will directly translate into variability in permeability. Focusing on the 8 participants who carried out 1D saturated tests and submitted permeability data passing all outlier tests (Table 6), the viscosity is on average:

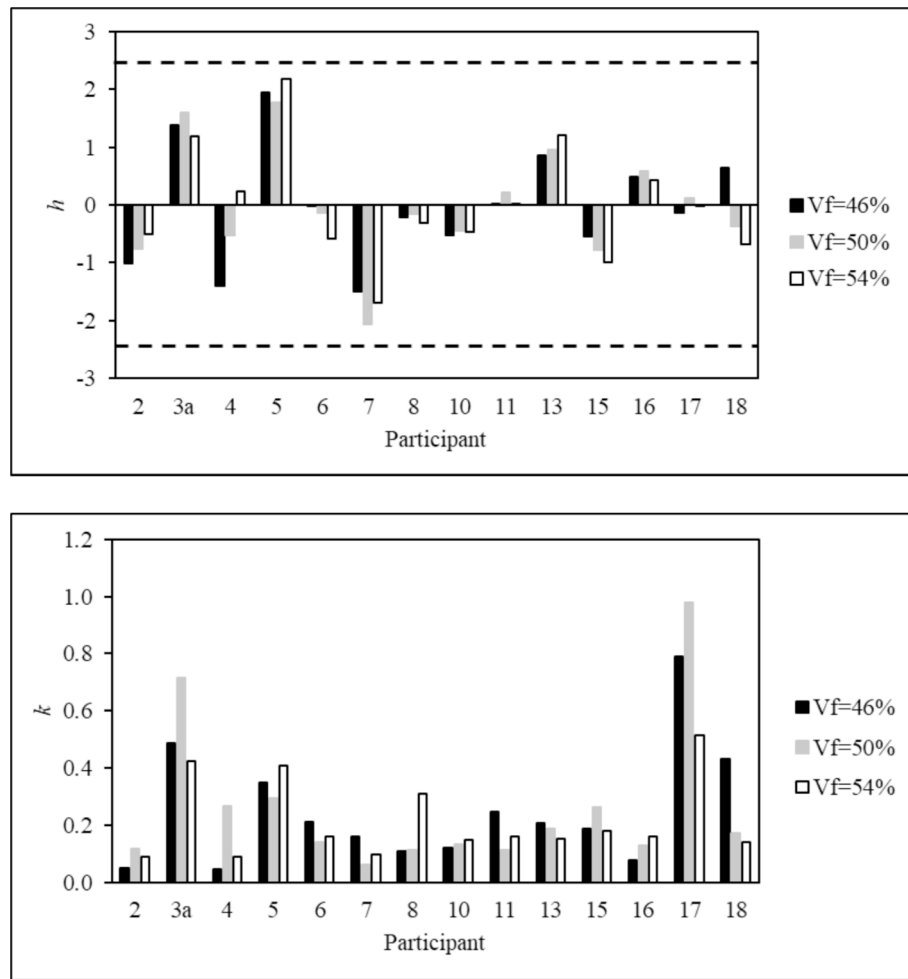


**Fig. 7.** Consistency measurements  $h$  and  $k$  after exclusion of unsaturated, 3D testing, and inverse  $K_z(V_f)$  relationships, and one outlier. Dashed line represents outlier threshold.

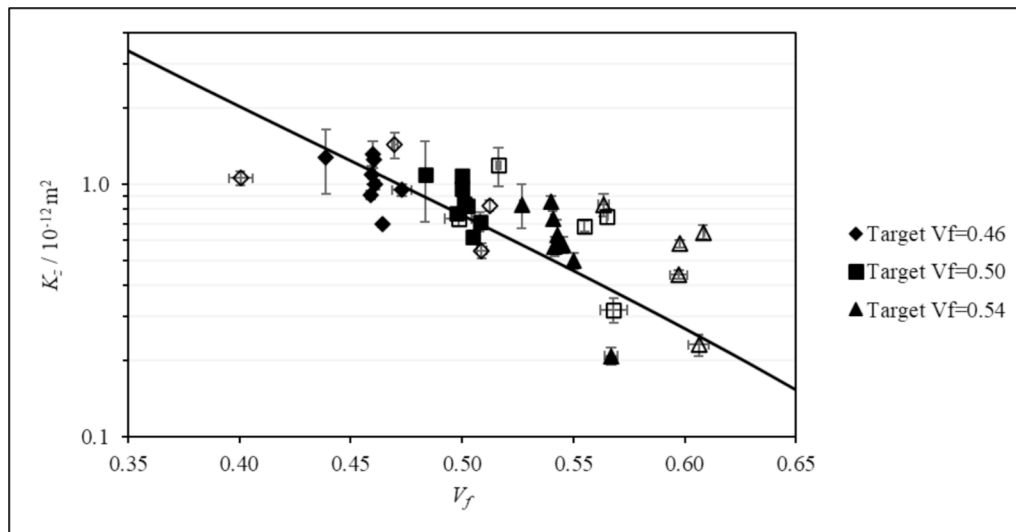


**Fig. 8.** Data points remaining after applying the Thompson-Tau test to bins with  $\Delta V_f = 0.04$ ; solid and hollow markers respectively denote compliance and non-compliance with the guidelines. The solid line indicates a KC fit curve with  $k_0 = 1.51 \times 10^{-12} \text{ m}^2$ ; the coefficient of correlation is  $R^2 = 0.895$ .

- within  $\pm 10\%$  of the reference for 6 participants,
- between 10 % and 20 % higher for one participant,
- between 20 % and 30 % higher for one participant.

As all the viscosity values deviating from the reference values were on average generally higher than the reference (with one exception), this could induce a difference in the average permeability after

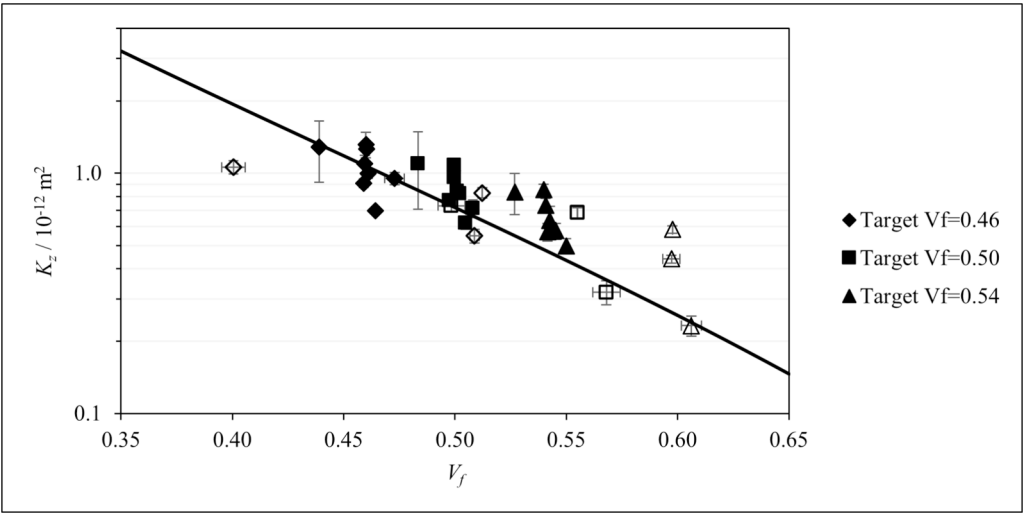


**Fig. 9.** Data points remaining after applying the Thompson-Tau test to KC coefficients for each individual data series; solid and hollow markers respectively denote compliance and non-compliance with the guidelines. The solid line indicates a KC fit curve with  $k_0 = 1.44 \times 10^{-12} \text{ m}^2$ ; the coefficient of correlation is  $R^2 = 0.917$ .

**Table 6**  
Results of outlier analysis. Shaded cells indicate data sets obtained in tests complying with the guidelines and passing all outlier tests.

Test series	Compliance	Pass ASTM 1	Pass ASTM 2	Pass Ttau bins	Pass Ttau KC
1	N	N			
2	Y	Y	Y	Y	Y
3a	N	Y	Y	Y	N
3b	N	Y			
4	N	Y	Y	Y	Y
5	N	Y	Y	N	N
6	Y	Y	Y	Y	Y
7	Y	Y	Y	N	N
8	Y	Y	Y	Y	Y
9a	N	N			
9b	Y	N			
10	Y	Y	Y	Y	Y
11	Y	Y	Y	Y	Y
12	N	N	N	N	N
13	N	Y	Y	Y	Y
14	Y	Y			
15	N	Y	Y	Y	Y
16	Y	Y	Y	Y	Y
17	Y	Y	Y	Y	Y
18	Y	Y	Y	Y	Y
19	N	N			

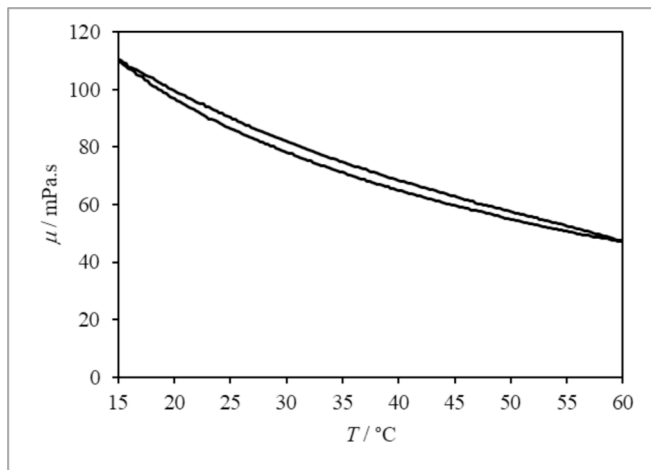


Fig. 10. Reference curve for the viscosity,  $\mu$ , of Xiameter PMX-200 Silicone Fluid 100 cs as a function of temperature,  $T$ . Lower  $\mu$  values correspond to the upward temperature ramp, higher values to the downward ramp.

application of Eq. (2). For the 14 “Pass ASTM 2” (in Table 6) data sets, the KC model was fitted to all data points, generating a  $k_0$  constant for each participant. This is the same as was done in the second Thompson-Tau analysis. This constant was then used as the result value for a  $t$ -test for significant difference in means, by comparison of those participants who stayed within 10 % of the viscosity reference, and those who did not. Although both conditions showed a normal distribution of data by the Shapiro-Wilk test, the  $t$ -test resulted in failure to reject the null hypothesis at a 95 % confidence level, i.e. that there was no significant difference in the means. On the other hand, of those 14 data sets, only four met the >10 % deviation condition, so the small data sampling for the “deviation” condition may contribute to this result, and a larger sample size may have still resulted in a significant difference in the resulting measured permeability.

### 5.3. Effect of experimental set-up

A  $t$ -test for significant difference in means (as used in the analysis of the viscosity variation) was also used for statistical analysis of which experimental set-up variables had a significant effect on the resulting permeability. The variables tested were rig closure method, edge-sealant method, tool thickness control, tool thickness measurement, flow measurement method, and overall compliance with the test specifications. Details of the rig closure methods have been provided in the [supplementary files](#). The KC fit constants were each divided into two bins for each parameter: 1) the most used condition, e.g. bolts for rig closure, and 2) anything besides that. All other parameter variables were excluded from analysis due to low variation, e.g. all remaining data sets used 1D saturated setups, and 12 of the 14 (data sets analysed in the previous section) used constant pressure instead of constant flow rate.

With the given sample size, the Shapiro-Wilk test for normality was first run on each bin's values. All showed a normal distribution with a 95 % confidence interval. A two-sample  $t$ -test was then performed to determine if there is a significant difference between the means of the two bins for each category. The only parameter which showed a significantly different mean at a 95 % confidence value, was the flow measurement method. When using mass loss from the pot containing the test fluid, the resulting KC fit constant is lower than when using any other method ( $1.46 \times 10^{-12} \text{ m}^2$  compared to  $1.85 \times 10^{-12} \text{ m}^2$ ). At the 90 % confidence value, the tool thickness control also showed a significant difference in means, using spacers resulted in a higher KC fit constant than anything else.

Note that any of the set-up variables can still have a relevant influence on the measurement outcome, even if no statistical significance is

proven by this analysis. The data set is relatively small and goes together with a high number of superimposing variations, making the data noisy and preventing a clear view on the effect of single parameters. Also note that this analysis does not evaluate which parameters result in higher or lower scatter, but which parameter settings result in a higher or lower result. These results suggest that there may be some modest influence in the relative magnitude of the permeability from some of the experimental parameters. In conclusion, any standardisation effort must still take into account all of the aforementioned variations and strive for minimisation of any possible differences.

### 5.4. Further comments

When carrying out 1D experiments, the fluid injection can either be set to a fixed flow rate or fixed injection pressure. There is no known influence on measurement of the permeability caused by which of these two parameters is fixed. During such experiments, however, it must be ensured that a steady state has been achieved (i.e. constant flow rate and pressure difference) prior to commencement of data recording. Limitations for pressure variations have been outlined in ISO 4410:2023, which can be used as guidance for out-of-plane testing [18].

In 1D flow experiments (saturated or unsaturated), the fabric specimens are typically compressed between two perforated platens. The permeability of the perforated platens was assessed by one participant. At the flow rates used in the experiments no measurable pressure drop was found in the presence of the platens (without fabric specimen). Based on the diameter of the holes, the permeability of the platens was estimated as  $10^{-6} \text{ m}^2$ , which is several orders of magnitude greater than the specimen permeabilities. Similar values will apply to the platens of other participants where the hole diameters were generally in the order of millimetres.

Yang et al. [35] suggested that the pores in the perforated platens induce tortuosity in the flow paths which could affect the measured permeability. For all participants in this study (using 1D set-ups), the diameter of holes in the platens and the width of material between the holes is in the order of magnitude of several millimetres. The width of fibre bundles in the fabric tested here was approximately 2 mm. Hence, the tortuosity in flow paths induced by the presence of the fibre bundles in the specimen is in the same order of magnitude as the tortuosity induced by the perforated platens. Making use of a correction factor as suggested by Yang et al. [35] does not seem necessary. The effect of the geometry of the compaction platens on the measured permeability has been discussed before [36]. However, in the previous benchmark exercise [9], no clear effect was observed.

The distance between the two perforated platens defines the cavity height and therefore calculation of the fibre volume fraction. It is important that this height remain constant throughout the test, without movement or deflection of the perforated platens. It is recommended that the cavity height be set with physical spacers unless a constant distance between the platens can be assured when set by other means.

When specimens for 1D flow experiments are prepared, any gaps between the specimen and the inner tool walls need to be sealed to avoid racetracking. If the application of sealant reduces the effective cross-sectional area available for flow, the true cross-sectional area is to be taken into account in permeability calculation. As an example, a reduction in diameter by 2 mm (1 mm around the specimen edge) for a circular specimen with the recommended diameter of 100 mm results in a reduction of the cross-sectional area by 4 %. This is of particular relevance if low-viscosity sealants are used, which may wick deep into the specimen. If a quantification of the true cross-sectional area is not possible, the specimen is to be discarded.

Table 3 shows that information on the experimental setup is missing for participant 12 who was identified as an outlier by significant margins compared with other participants. As the guideline requesting complete information to be provided was not followed, it is not possible to isolate the source of the deviation in the results. This highlights the need for



proper recording, for which the guidelines should be outlined in any future test standard.

In the guidelines provided to the participants, some recommendations had been made for specimen storage (temperature and humidity control). These are critical for resins and prepreps as exposure to heat and humidity may affect the polymer properties but are thought to be not critical for dry fabrics. However, it is essential that the tested material can acclimatise to the conditions in the testing environment. Hence, it can be recommended that the test set-up, the reinforcement specimens and the test fluid are stored at laboratory conditions for at least 24 h before testing starts.

### 5.5. Comparison with excluded datasets

The unsaturated 3D methodology (used by participants 1 and 19) has potential advantages compared to the 1D methods: determination of all three components of the permeability tensor in one test, no need to seal the cut sample edges due to radial flow (Fig. 2), and no risk of pressure drop complications due to hole pattern. The intra-lab consistency shown in this study by the 3D methods was fair, i.e. not the worst, but on the low end compared to 1D saturated method data sets (Fig. 5). The additional flow directions, in addition to the wetting complications typical to any unsaturated test, are thought to be the reason for slightly more scatter in results. The inter-lab consistency was fairly consistent with many of the 1D method data sets, except for one participant's (#19) data at 46 % fibre content. This exception was apparently caused by racetracking of the test fluid across the sample in-plane surface, due to low compression of the sample stack at that low fibre content. In this case of low fibre content, a 1D method may be better equipped to avoid racetracking due to forcing the flow through only the z-direction.

## 6. Conclusions

In this benchmark exercise, 19 participating laboratories submitted 21 measured datasets on the through-thickness permeability of a glass fibre non-crimp fabric. To minimise the variability in permeability data, detailed guidelines for the experiments were provided to the participants.

After the data sets from 3D tests, from 1D unsaturated tests and implausible data are excluded from the analysis, application of statistical methods for data evaluation showed that compliance with the provided guidelines gives a high chance at not being identified as an outlier. The probability of being consistent with the other data sets (not flagged as an outlier) is 50 % for data sets that were non-compliant with the provided guidelines, whilst it is 89 % for compliant data sets. Hence, it can be recommended to adhere to the proposed guidelines to maximise the chance of obtaining consistent data between laboratories. This also shows that the guidelines developed provide a suitable basis for standardisation.

When first including all data sets, the Kozeny-Carman model fit to all data yielded a low correlation value,  $R^2 = 0.255$ . When including only data sets that passed all outlier screening methods, the  $R^2$  value improves to 0.917. Whilst this does not prove the validity of the KC model, it allows to evaluate the data with a single variable (the fit of the model) instead of two. Assuming the KC model is a valid relationship between fibre volume content and permeability, then compliance with these test standards makes more believable data.

Based on the statistical analyses of the data, the following recommendations can confidently be made for repeatable and reproducible measurement of the out-of-plane permeability ( $K_z$ ) and will be included in the proposal for a test standard:

- The test method should be 1D saturated.
- Specimens should be tested at three defined fibre volume fractions,  $V_f$ . The recommended target values are 45 %, 50 % and 55 %.
- Five test repeats should be carried out.

- Specimens should consist of a fabric stack of no less than 10 and no more than 20 individual layers, all stacked with equal orientation (unless specimens of a specific lay-up sequence are to be tested).
- Specimens should have an edge length (if square) or diameter (if round) in the order of 100 mm.
- Specimens should be cut with a precise method (such as a CNC cutter or die cutter).
- Pressure and flow rate should be measured independently of set (target) values.
- Participants should employ an edge-sealing procedure, such as the use of a sealant paste or O-ring.
- The pressure differential,  $\Delta p$ , between the top and bottom surface of the specimens should be between 100 kPa and 200 kPa during testing.
- A record of all test parameters must be provided with the test results.

## CRediT authorship contribution statement

**A.X.H. Yong:** Writing – original draft, Project administration, Methodology, Investigation, Formal analysis, Data curation, Conceptualization. **A. Endruweit:** Writing – original draft, Methodology, Investigation, Formal analysis. **A. George:** Writing – original draft, Investigation, Formal analysis. **D. May:** Writing – original draft, Methodology, Investigation, Formal analysis. **Y.A. Aksoy:** Investigation. **M. A. Ali:** Investigation. **T. Allen:** Investigation. **P. Baral:** Investigation. **C. Betteridge:** Investigation. **C. Brauner:** Investigation. **B. Caglar:** Investigation. **A. Chiminelli:** Investigation. **D. Cracknell:** Investigation. **L. Dame:** Investigation. **J. Dittmann:** Investigation. **C. Dransfeld:** Investigation. **S. Drapier:** Investigation. **J.A. García Manrique:** Investigation. **E. Garrigou:** Investigation. **A. Guilloux:** Investigation. **P. Hubert:** Methodology, Investigation. **J. Ivens:** Investigation. **J. Janzen:** Investigation. **T. Khan:** Investigation. **H. Kikuta:** Conceptualization. **K. Kind:** Investigation. **M. Laspalas:** Investigation. **J. Lee:** Investigation. **X. Liu:** Investigation. **M. Lizaranzu:** Investigation. **S.V. Lomov:** Methodology, Investigation. **K. Masania:** Investigation. **V. Michaud:** Investigation. **P. Middendorf:** Supervision. **S. Miguel:** Investigation. **J. Muñoz:** Investigation. **S.S. Narayana:** Investigation. **C.H. Park:** Investigation. **G. Pedoto:** Investigation. **A. Pisupati:** Investigation. **D. Sayinbas:** Investigation. **P. Sousa:** Investigation. **M. Sozer:** Investigation. **J. Staal:** Investigation. **M. Steinhardt:** Investigation. **H. Teixido:** Investigation. **R. Umer:** Investigation. **J.D. Vincent:** Investigation. **V. Werlen:** Investigation. **O. Yuksel:** Investigation.

## Declaration of competing interest

The authors declare that they have no known competing financial interests or personal relationships that could have appeared to influence the work reported in this paper.

## Acknowledgements

The authors thank Saertex GmbH for supplying the materials used in this exercise free of charge. ITA participation in this benchmark has been possible thanks to the support of the European Regional Development Fund (ERDF) for Aragon region (Spain).

## Appendix A. Supplementary data

Supplementary data to this article can be found online at <https://doi.org/10.1016/j.compositesa.2024.108630>.

## Data availability

Data will be made available on request.

## References

- [1] Potter K. Resin transfer moulding. London: Chapman and Hall; 1997.
- [2] Rudd CD, Long AC, Kendall KN, Mangin CGE. Liquid moulding technologies. Cambridge: Woodhead Publishing; 1997.
- [3] Parnas RS. Liquid composite moulding. Munich: Hanser Verlag; 2000.
- [4] Darcy H. Les Fontaines Publiques de la Ville de Dijon. Paris: Victor Dalmont; 1856.
- [5] Yun M, Sas H, Simacek P, Advani SG. Characterization of 3D fabric permeability with skew terms. *Compos Part A-Appl S* 2017;97:51–9.
- [6] Arbter R, Beraud JM, Binetruy C, Bizet L, Bréard J, Comas-Cardona S, et al. Experimental determination of the permeability of textiles: a benchmark exercise. *Compos Part A-Appl S* 2011;42(9):1157–68.
- [7] Vernet N, Ruiz E, Advani S, Alms JB, Aubert M, Barbuski M, et al. Experimental determination of the permeability of engineering textiles: Benchmark II. *Compos Part A-Appl S* 2014;61:172–84.
- [8] May D, Aktas A, Advani SG, Endruweit A, Fauster E, Lomov SV, et al. In-plane permeability characterization of engineering textiles based on radial flow experiments: a benchmark exercise. *Compos Part A-Appl S* 2019;121:100–14.
- [9] Yong AXH, Aktas A, May D, Endruweit A, Advani S, Hubert P, et al. Out-of-plane permeability measurement for reinforcement textiles: a benchmark exercise. *Compos Part A-Appl S* 2021;141.
- [10] Yong AXH, Aktas A, May D, Endruweit A, Lomov SV, Advani S, et al. Experimental characterisation of textile compaction response: a benchmark exercise. *Compos Part A-Appl S* 2021;142.
- [11] Weitzenboeck JR, Shenoi RA, Wilson PA. A unified approach to determine principal permeability of fibrous porous media. *Polym Compos* 2002;23(6):1132–50.
- [12] Sharma S, Siginer DA. Permeability measurement methods in porous media of fiber reinforced composites. *Appl Mech Rev* 2010;63(2):020802.
- [13] Parnas RS, Howard JG, Luce TL, Advani SG. Permeability characterization. Part 1: a proposed standard reference fabric for permeability. *Polym Compos* 1995;16(6):429–45.
- [14] Lundström TS, Stenberg R, Bergström R, Partanen H, Birkeland PA. In-plane permeability measurements: a Nordic round-robin study. *Compos Part A –Appl S* 2000;31(1):29–43.
- [15] Berg DC, Fauster E, Abliz D, Grössing H, Meiners D, Schledjewski R, Ziegmann G. Influence of test rig configuration and evaluation algorithms on optical radial-flow permeability measurement: a benchmark exercise. In: *Proc. of ICCM20*; 2015.
- [16] Grössing H, Becker D, Kaufmann S, Schledjewski R, Mitschang P. An evaluation of the reproducibility of capacitive sensor based in-plane permeability measurements: a benchmarking study. *Express Polym Lett* 2015;9(2):129–42.
- [17] Becker D, Grössing H, Konstantopoulos S, Fauster E, Mitschang P, Schledjewski R. An evaluation of the reproducibility of ultrasonic sensor-based out-of-plane permeability measurements: a benchmarking study. *Adv Manuf Polym Compos Sci* 2016;2(1):34–45.
- [18] ISO 4410:2023. Test methods for the experimental characterization of in-plane permeability of fibrous reinforcements for liquid composite moulding. Geneva: International Organisation for Standardisation; 2023.
- [19] Pillai KM. Unsaturated flow in liquid composite molding processes: a review and some thoughts. *J Compos Mater* 2004;38(23):2097–118.
- [20] Michaud V. A review of non-saturated resin flow in liquid composite moulding processes. *Transport Porous Med* 2016;115(3):581–601.
- [21] Dungan FD, Sastry AM. Saturated and unsaturated polymer flows: microphenomena and modeling. *J Compos Mater* 2002;36(13):1581–603.
- [22] Hoes K, Dinescu D, Sol H, Parnas RS, Lomov S. Study of nesting induced scatter of permeability values in layered reinforcement fabrics. *Compos Part A-Appl S* 2004;35(12):1407–18.
- [23] Song YS, Heider D, Youn JR. Statistical characteristics of out-of-plane permeability for plain-woven structure. *Polym Compos* 2009;30:1465–72.
- [24] Swery EE, Allen T, Comas-Cardona S, Govignon Q, Hickey C, Timms J, et al. Efficient experimental characterisation of the permeability of fibrous textiles. *J Compos Mater* 2016;50(28):4023–38.
- [25] Binetruy C, Hilaire B, Pabiot J. Influence of fiber wetting in resin transfer molding: scale effects. *Polym Composite* 2000;21(4):548–57.
- [26] Willenbacher B, May D, Mitschang P. Out-of-plane capillary pressure of technical textiles. *Compos Part A- Appl S* 2019;124:105495.
- [27] Wu CH, Wang TJ, Lee LJ. Trans-plane fluid permeability measurement and its applications in liquid composite molding. *Polym Composite* 1994;15(4):289–98.
- [28] Endruweit A, Luthy T, Ermanni P. Investigation of the influence of textile compression on the out-of-plane permeability of a bidirectional glass fiber fabric. *Polym Composite* 2002;23(4):538–54.
- [29] Becker D, Mitschang P. Measurement system for on-line compaction monitoring of textile reaction to out-of-plane impregnation. *Adv Compos Lett* 2014;23(2):32–6.
- [30] Mekic S, Akhatov I, Ulven C. A radial infusion model for transverse permeability measurements of fiber reinforcement in composite materials. *Polym Composite* 2009;30:907–17.
- [31] Carman PC. Fluid flow through granular beds. *T I Chem Eng-Lond* 1937;15:150–6.
- [32] Gebart BR. Permeability of unidirectional reinforcements for RTM. *J Compos Mater* 1992;26(8):1100–33.
- [33] Brusckie MV, Advani SG. Flow of generalized Newtonian fluids across a periodic array of cylinders. *J Rheol* 1993;37(3):479–98.
- [34] ASTM E691. Standard practice for conducting an interlaboratory study to determine the precision of a test method. West Conshohocken, PA: ASTM International; 2011.
- [35] Yang B, Huang W, Causse P, Béguin C, Wang J, Trochu F. On the design of test molds based on unidirectional saturated flows to measure transverse permeability in liquid composite molding. *Polym Composite* 2022;43:2234–51.
- [36] Graupner R, Drechsler K. Quantitative transversal permeability testing - challenges and enhancements. In: *The 14th International Conference on Flow Processing in Composite Materials*, Lulea; 2018.